JACS
JOURNAL OF THE AMERICAN CHEMICAL SOCIETY

Communication

pubs.acs.org/JACS

Self-Assembled Dipole Nanolasers

Kevin G. Stamplecoskie, Michel Grenier, and Juan C. Scaiano*

Department of Chemistry and Centre for Catalysis Research and Innovation, University of Ottawa, 10 Marie Curie, Ottawa, Ontario K1N 6N5, Canada

Supporting Information

ABSTRACT: Visible light excitation of silver nanoparticles in the presence of polymerizable monomers and selected dyes triggers the self-assembly of nanolasers in a synthetically simple process. The new nanolasers incorporate a thin, fully organic gain medium that allows the tuning of the core absorption to a selected dye, or of the dye to a preselected core material. This versatile synthesis of surface plasmon lasers, or "spasers", has unique simplicity and enables spatial and temporal control of the nanolaser fabrication process.

In 2009, Noginov et al. reported the first synthesis of a nanoparticles/dye assembly that could act as a "spaser", or surface plasmon amplification by stimulated emission of radiation.[1] The elaborate assembly consisted of gold nanoparticles and a buffering silicate layer surrounded by a high concentration of dye trapped in a silica shell around the particle. This landmark work would benefit from simpler synthetic strategies that could allow incorporating these components into nanophotonic optoelectronics.[2]

A body of experimental evidence for the coupling of surface plasmon polaritons (SPPs) with emitters for optical gain, mostly performed for the coupling of long-range SPP (LRSPPs) with gain media, provides the foundation for the development of dipole nanolasers. The first reported use of LRSPP for gain was in 1979 by Plotz et al., who described amplified total reflection for a metal slab in contact with glass at varying angles.[3] Sudarkin and Demkovic later suggested lasing from SPPs based on Plotz's work.[4] Siedel et al. first demonstrated spontaneous emission of SPPs by flowing solutions of cresol violet and Rhodamine 101 over a silver film, where nonzero changes in reflectance as a function of excitation angle were attributed to stimulated emission of the SPPs through coupling with the dye as a gain medium.[5] These contributions are a small sampling of the research devoted to understanding the coupling of emitters/dipoles with SPPs. Stockholm and others had theoretically predicted spontaneous emission of surface plasmons for similar plasmonic structures.[6,7] The particles must be in close proximity to the emitters in the gain medium so that the plasmon field (which decays rapidly with distance from the surface, like all evanescent fields) overlaps with the emitters. The emission spectrum of the dye must have significant overlap with the plasmon resonance, such that the two can couple strongly.

A brief description of the mechanism of spontaneous emission from dipole nanolasers is provided here, but for an in-depth understanding one should refer to theoretical works by Stockman, Rosenthal and Ghannam, and Noginov et al.[2,6−8] A laser needs three fundamental components—a pump, a resonator (or feedback), and a gain medium, usually provided by a dye or semiconductor material. In the dipole nanolaser, metal nanoparticles (NPs) can serve as the resonator, confining light of a given frequency. The gain medium can consist of dye molecules. Increased excitation intensities (pump) result in stronger enhanced near-field effects and, therefore, drastically stronger excitation of the gain medium. This feeds energy through strong resonant coupling back into the surface plasmon, providing a feedback mechanism, as illustrated in Figure 1. Above a certain pumping threshold of excitation, an instability arises in surface plasmon excitation (resulting from energy transfer from the gain medium), and emission of coherent surface plasmon is observed,[2] with periodic fluctuations of emission decay as a characteristic spaser feature.

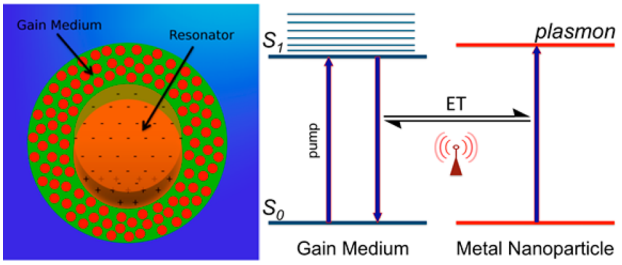

Figure 1. Left: Illustration of an excited plasmon behaving as an antenna to enhance excitation of neighboring dye molecules in the gain medium, that pump energy through energy transfer (ET) back into the plasmon mode, thus stimulating the emission from the highly excited plasmon. Right: Simplified energy level diagram of relevant excited-state interactions.

It has been theoretically predicted that a single dipole interacting with a plasmon can produce the same effect, which was later disproven, as it was shown that many emitters in the gain medium are required to realize spontaneous emission of surface plasmons.[2,9] It was also predicted that a quantum dot (QD) and metal NP bound together and with good overlap of the QD emission and metal particle plasmon could produce the dipole nanolaser effect, but this was also questioned due to the small separation of dipoles in such a system.[2,9] A recent report builds an epitaxially grown 0.48 μm low-temperature nanolaser.[10] Therefore, while experimentally involved, the spaser

Received: November 16, 2013
Published: February 10, 2014

   dx.doi.org/10.1021/ja411696r | J. Am. Chem. Soc. 2014, 136, 2956−2959

reported by Noginov et al.[1] remains the only reported room-temperature spaser of true nanoscale dimensions.

Lithographic approaches are used for electronic chip design since they offer great spatial control of generating polymer features. The drawback is that traditional lithography has fundamental limitations in minimum feature size.[11] Polymerization on the surface of NPs, however, can be controlled by plasmon excitation and generate sub-diffraction-sized features.[12,13] This technique is used here to trap dye molecules around silver nanoparticles (AgNPs) and, in doing so, form dipole nanolasers. The surrounding matrix (not polymerized) can be removed by selective solubilization after polymerization, in typical lithography-type processing. These dipole nanolasers are potentially important for optoelectronics, especially due to the light-induced self-assembly approach shown here.

Plasmon excitation is also known to relax predominantly by photothermal heat release (thermoplasmonics).[14,15] Radical polymerization can also be initiated by plasmon excitation, but since dyes with extended π conjugation are known to react with radicals, significant bleaching of dyes results.[16] Our two examples for self-assembly of dipole nanolasers use the heat generated by plasmon excitation for formation of nylon-6 shells around decahedral AgNPs, as well as selective radical polymerization around Ag nanoplates to form cross-linked polymer shells. Due to the reaction of radicals with dyes, the thermal route to polymerization provides more robust nanolasers.

In our first example, we trap coumarin 6 (C6) as the dye molecule in self-assembled nylon-6 features around the AgNP, as shown in Scheme 1; for simplicity C6 is omitted from the scheme as it plays a passive role in the synthesis reaction, but it is embedded in the polymer to later act as the active gain component.

Scheme 1. Plasmon Excitation Used To Deliver Localized Heat Polymerizing Caprolactam to Nylon-6 (Brown Circle around Pentagon) and Trapping C6 around Decahedral Nanoparticles

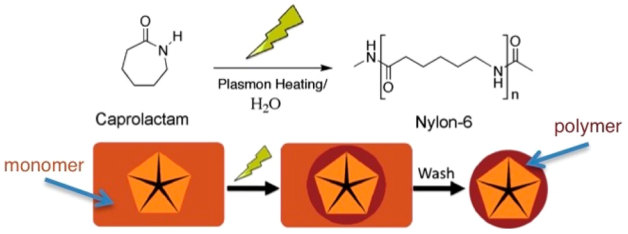

Typical solutions containing <1% Ag decahedra, 2% C6, and 50% caprolactam in acetonitrile were spin-coated at 2500 rpm onto 1-in. quartz disks and irradiated with a 465 nm LED to form a polymer shell through plasmon heating (see Supporting Information (SI) for experimental setup for LED irradiation). The reaction in the film was monitored by UV−vis spectroscopy, showing that C6 (in the nylon-6 shell) is retained on the films after plasmon heating, even after the unreacted monomer has been removed by washing.

A second approach involving radical polymerization to form Ag nanoplate lasers with Eosin Y (EY) is shown in the SI. This methodology takes advantage of conventional lithographic techniques, where a solubility switch is provided by light-induced polymerization and the excess monomer is removed in a washing step. Both approaches lead to particles that were examined with fluorescence lifetime imaging microscopy (FLIM) and show bright spots where the dipole nanolasers are retained and dark areas around the spots where the nonpolymerized film has been removed by washing (see Figures 2 and S5).

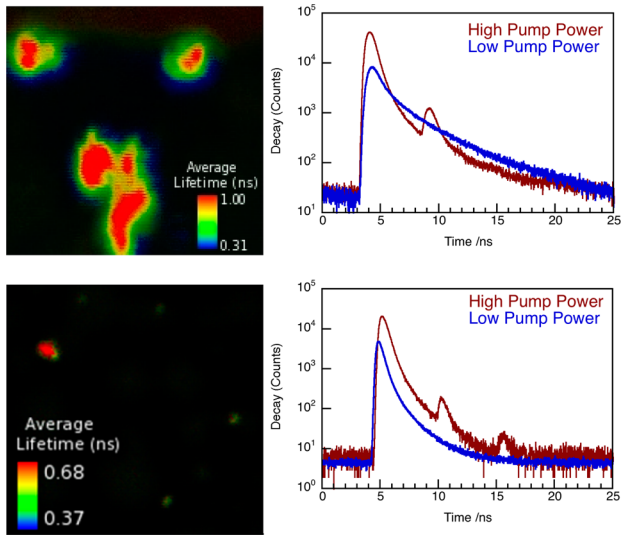

Figure 2. Top: FLIM image of decahedral AgNPs with coumarin-6 embedded in a nylon-6 shell around the NPs, as well as emission lifetime profile above (red) and below (blue) the pumping threshold for lasing. Bottom: Similar FLIM image and lifetime traces above (red) and below (blue) the threshold for lasing of Ag nanoplates with a cross-linked methacrylate polymer used to trap Eosin Y molecules around the NP. The FLIM image for the C6/decahedra lasers is 2.8 μm wide, and that for the EY/nanoplates lasers is 18.48 μm wide.

The emission spectra for both dipole nanolaser assemblies (see Figure S4b) do not show a narrow but intense emission spike for the spasing mode at either high- or low-power excitation conditions; this is different from the work by Noginov et al.[1] The emission bandwidth is intimately related to the excitation pulse duration and energy, which give a lower peak pulse intensity here.[6] Rosenthal et al.[7] show that this avalanche of emission with a broad spectrum is in fact expected for dipole nanolasers, and only significantly above the lasing threshold, with multiple emitters in the gain medium, and with spatial separation between the emitter dipole and the plasmon, does the emission spectrum narrow as seen by Noginov.[1]

One of the critical requirements for laser action in these NPs is that the particle plasmon absorption and dye overlap both spatially and spectrally (with the emission of the dye). The spatial overlap achieved is shown in the scanning electron microscopy (SEM) images (*vide infra*, Figures 3 and S3), since the dye is trapped in the layer of polymer around the NP. From the SEM images of the particles, the polymer layer comprises approximately 30% of the NP by volume. The spectral overlap is illustrated in Figure 3 for both dipole nanolaser systems, where it is important to note that the dye emission and NP plasmon have the required energies for favorable coupling (more overlap in the Ag decahedra/C6 particles).

The highest possible resolution for the images in Figure 2 is limited by optical diffraction. Therefore, it is not possible to discern from the images whether or not individual particles or assemblies are responsible for lasing. However, the same solutions used for spin coating and making decahedra/C6

dx.doi.org/10.1021/ja411696r | J. Am. Chem. Soc. 2014, 136, 2956−2959

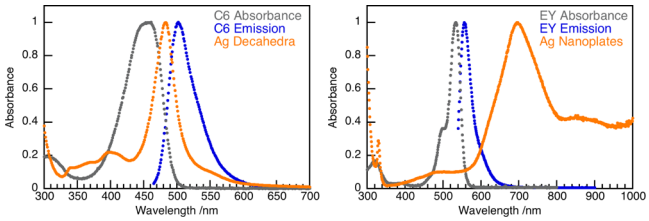

Figure 3. Left: UV−vis absorption spectra for C6 and Ag decahedra in solution, and emission spectrum for C6 as indicated. Right: UV−vis absorption spectra for EY and Ag nanoplates in solution, and emission spectrum for EY as indicated.

nanolasers can be directly excited with a 465 nm light-emitting diode (LED) to form individual decahedral particles with polymer shells as shown in Figure 4. When spin-coated onto

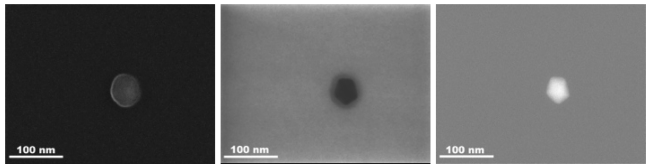

Figure 4. Back-scattering SEM (left), TEM (middle), and COMPO (right) images of the same single decahedral AgNP with a nylon-6 shell.

glass slides, these already pre-assembled nanolasers exhibit the same lasing properties as those made in films (data not shown). More importantly, there were no bright spots during fluorescence imaging of these pre-assembled particles that did not show the lasing behavior at high excitation powers. These results support the claim that individual particles can act as lasers, as it would be very unlikely to form exclusively aggregates from a suspension that is known to contain individual particles; further, these particles remain largely monomeric when deposited on TEM grids.

For FLIM measurements, above and below the pumping threshold for lasing, two arrangements were used for the instrumental setup (Scheme 2). For decahera/C6 nanolaser

Scheme 2. Attenuation Techniques To Achieve Lasing (B) or Normal Emission (A)[a]

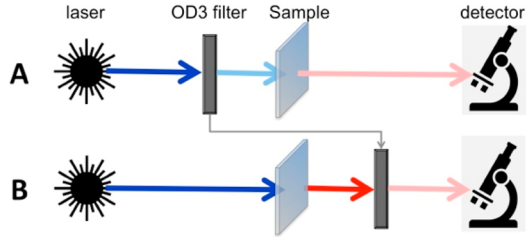

[a]In both arrangements signal is attenuated by ×1000, but in B it is achieved following high-power sample excitation.

assemblies, 440 nm laser excitation was used, and for nanoplate/EY assemblies, 530 nm excitation was used. Further information on the pump power conditions can be found in the SI. The overall beam intensity was held constant in both cases, receiving the same total attenuation (OD3, or ×1000) before reaching the detector, but for pumping above the threshold, the samples experienced 1000× the excitation intensity. It is important to note that the excitation power from the laser is not changed for either high- or low-power excitation; similarly, the detection system is identical as well. The attenuation in the beam path is simply moved from before/after the sample. The integrated intensity of the lifetime trace is stronger when above the lasing threshold, as expected, since the whole system is based on gain of total emission (Figure 2). Also important to note is that neither of the decay profiles fit well to a single exponential decay, whereas C6 alone in a caprolactam film does fit monoexponential kinetics (see SI). This difference is another indication that the polymer films are in fact a shell-like coating that traps the dye moleculs near the AgNPs, since the energy transfer from the dye molecules to the AgNPs results in a non-monoexponential decay of the dye emission.[14] A characteristic signature of this type of stimulated emission is the periodic fluctuation observed in emission vs time traces.[7,8] Note the presence of this signature feature in Figure 2 (right).

The chemistry for making nylon-6 features around decahedral particles described above for thin films can also be performed directly with the solutions used for spin coating (see SI), with polymer shells grown on particles upon plasmon excitation. The colloidal solutions of particles/nanolasers with polymer shells could be centrifuged and resuspended several times in acetonitrile to remove unreacted caprolactam and the C6 fraction that was not trapped in the shell around the particles. Transmission electron microscopy (TEM), back-scattering SEM, and energy loss back-scattering COMPO SEM images of a single particle, shown in Figure 4, illustrate the polymer shell on the decahedral particle. The back-scattering SEM image in Figure 4 (left) shows mostly the surface of the particle/shell, with only a slightly higher interaction of the electron beam with the metal center. TEM images, on the other hand (Figure 4, middle), show clearly the decahedral particle core with a lighter polymer shell. COMPO images like the one shown in Figure 4 (right) give bright spots for regions with energy loss for the electron beam that is due to heavy elements like Ag, thus showing the Ag core of the particles. The particles were homogeneously coated with nylon shells, as seen in images of multiple particles with nylon-6 shells (see the SI). The average edge length of a decahedral particle used here is ∼30 nm, and the shell thicknesses were very uniform throughout samples at ∼9 nm. The shell comprises ∼30% of the nanolaser volume and contains 2% by weight C6, which corresponds to ∼1160 molecules surrounding each particle.

In the experiments with EY, the dye emission does not have a large spectral overlap with the plasmon absorption of the Ag nanoplates (Figure 2, right). This combination was chosen to minimize direct dye absorption during photochemical synthesis, such that the dye forms radicals selectively in the enhancement region around the particle surface (Scheme S5).[12] This synthetic condition requires a large Stokes shift for dye emission to overlap strongly with the Ag plate plasmon absorption. Even with imperfect overlap of the Ag plate plasmon and the dye emission, there is enough coupling to result in lasing, as evidenced by the multiple peaks in the emission lifetime trace at high pump powers; notice in particular the third maximum in Figure 2 (bottom), a desirable signature for plasmonic nanolasers.

Metal oxide field effect transistors (MOSFETs) are the active gain component that has been the enabling feature for conventional microelectronics. An active gain component for optoelectronics, such as the dipole nanolaser, could bring optoelectronics forward as a competitive technology.[2] When pumping levels are low the spaser acts as a transistor in the "off

dx.doi.org/10.1021/ja411696r | J. Am. Chem. Soc. 2014, 136, 2956−2959

state", analogous to a field effect transistor with no current flowing. However, when the pump pulse occurs, net amplification and a coherent plasmon are generated, giving stimulated emission, which is analogous to the "on" in a conventional transistor. This becomes clear when looking at the lifetime traces for emission of a spaser shown here (Figure 2 and Scheme 2), where below the pumping threshold for lasing the dye shows a normal decay, whereas above this threshold there is a delayed stimulated emission, which can serve as the signal when working as a nanoamplifier. Therefore, in time-gated operation, the spaser can in fact behave as a nanoamplifier.

In summary, the seminal work by Noginov et al.,[1] assembling the spaser using Au/silica/dye core−shell nanoparticles, requires significant synthetic time and skill. We report here a simple self-assembly method for synthesizing dipole nanolasers with AgNPs and a gain medium. The technique uses visible light, such as LEDs, to induce self-assembly of polymer shells, which then spontaneously trap dye molecules around the particles as the gain medium. This technique uses optical synthesis of the particles/shells, which not only provides spatial and temporal resolution for synthesis but also is compatible with current photolithographic techniques. The self-assembly strategy uses fundamental properties of metal NPs, the heat released upon plasmon excitation, and the electromagnetic field enhancement in close proximity to excited metal particle surfaces. Recent advances in AgNP research have led to a number of techniques to control the morphology, and therefore the optical properties, of various shapes of AgNPs with a diversity of surface functionalization.[17] These particles can therefore be selected for desired optical properties and combined with numerous dyes for optimizing the active gain using the techniques illustrated here. This work represents the first report of spasers made in a simple, light-induced self-assembly process and, as such, provides a means to fabricating coherent plasmon fields for optoelectronics with the spatial and temporal control of advanced lithography.

■ ASSOCIATED CONTENT

Supporting Information

Experimental details for synthesis of dipole nanolasers and fluorescence lifetime imaging experiments, as well as electron microscopy characterization of the synthesized nanolasers. This material is available free of charge via the Internet at http://pubs.acs.org.

■ AUTHOR INFORMATION

Corresponding Author

scaiano@photo.chem.uottawa.ca

Notes

The authors declare no competing financial interest.

■ ACKNOWLEDGMENTS

The Natural Sciences and Engineering Research Council (NSERC, Canada) supported this work through its Discovery, scholarships, and CREATE programs. Thanks are due to CFI (Canada) that funded the key tools used in this research.

■ REFERENCES

(1) Noginov, M.; Zhu, G.; Belgrave, A.; Bakker, R.; Shalaev, V.; Narimanov, E.; Stout, S.; Herz, E.; Suteewong, T.; Wiesner, U. *Nature* **2009**, *460*, 1110.
(2) Stockman, M. I. *J. Opt.* **2010**, *12*, 024004.
(3) Plotz, G. A.; Simon, H. J.; Tucciarone, J. M. *J. Opt. Soc. Am.* **1979**, *69*, 419.
(4) Sudarkin, A. N.; Demkovich, P. A. *Sov. Phys. Tech. Phys.* **1989**, *34*, 764.
(5) Seidel, J.; Grafström, S.; Eng, L. *Phys. Rev. Lett.* **2005**, *94*, 177401.
(6) Bergman, D. J.; Stockman, M. I. *Phys. Rev. Lett.* **2003**, *90*, 027402.
(7) Rosenthal, A.; Ghannam, T. *Phys. Rev. A* **2009**, *79*, 7.
(8) Noginov, M.; Fowlkes, I.; Zhu, G.; Novak, J. *J. Mod. Opt.* **2004**, *51*, 2543.
(9) Protsenko, I.; Uskov, A.; Zaimidoroga, O.; Samoilov, V.; O'reilly, E. *Phys. Rev. A* **2005**, *71*, 7.
(10) Lu, Y.-J.; Kim, J.; Chen, H.-Y.; Wu, C.; Dabidian, N.; Sanders, C. E.; Wang, C.-Y.; Lu, M.-Y.; Li, B.-H.; Qiu, X.; Chang, W.-H.; Chen, L.-J.; Shvets, G.; Shih, C.-K.; Gwo, S. *Science* **2012**, *337*, 450.
(11) Wallraff, G. M.; Hinsberg, W. D. *Chem. Rev.* **1999**, *99*, 1801. Deeb, C.; Ecoffet, C.; Bachelot, R.; Plain, J.; Bouhelier, A.; Soppera, O. *J. Am. Chem. Soc.* **2011**, *133*, 10535.
(12) Stamplecoskie, K. G.; Pacioni, N. L.; Larson, D.; Scaiano, J. C. *J. Am. Chem. Soc.* **2011**, *133*, 9160.
(13) Stamplecoskie, K. G.; Fasciani, C.; Scaiano, J. C. *Langmuir* **2012**, *28*, 10957. Deeb, C.; Ecoffet, C.; Bachelot, R.; Plain, J.; Bouhelier, A.; Soppera, O. *J. Am. Chem. Soc.* **2011**, *133*, 10535.
(14) Baffou, G.; Quidant, R. *Laser Photon. Rev.* **2013**, *7*, 171.
(15) Coronado, E.; Encina, E.; Stefani, F. *Nanoscale* **2011**, *3*, 4042. Haas, K. M.; Lear, B. J. *Nanoscale* **2013**, *5*, 5247. Fasciani, C.; Bueno Alejo, C. J.; Grenier, M.; Netto-Ferreira, J. C.; Scaiano, J. C. *Org. Lett.* **2011**, *13*, 204.
(16) Wu, C.-Y.; Kuo, C.-T.; Wang, C.-Y.; He, C.-L.; Lin, M.-H.; Ahn, H.; Gwo, S. *Nano Lett.* **2011**, *11*, 4256.
(17) Stamplecoskie, K. G.; Scaiano, J. C. *J. Am. Chem. Soc.* **2010**, *132*, 1825. Silvestrini, S.; Carofiglio, T.; Maggini, M. *Chem. Commun.* **2013**, *49*, 84.